Isomer and prompt spectroscopy of transplutonium nuclei

S.K. Tandel*
UM-DAE Centre for Excellence in Basic Sciences, Vidyanagari, Mumbai-400098, INDIA

The heaviest nuclei accessible to spectroscopic studies, in the transplutonium region, have been studied. K isomers in even-even nuclei ranging from Pu (Z=94) to Rf (Z=104) have been identified and their decay properties studied. In complementary work, rotational bands in several of these nuclei, including those built on K-isomeric states have been established to high spins. These experimental data have helped in constraining theoretical descriptions of the heaviest nuclei, and are expected to lead to more reliable predictions about the island of stability for superheavy nuclei.

1. Introduction

The extension of the periodic chart into unexplored regions of large atomic number Z has been an enduring pursuit in nuclear physics research. The stability of nuclei against fission is critically dependent on the delicate balance between the nuclear attractive interaction which gives the characteristic shell-correction energies, and the strong Coulomb replusion. Spectroscopic studies of shell-stabilized (Z≈100) nuclei offer valuable insight into several nuclear structure aspects, and in addition provide discriminating tests of theoretical approaches which predict the properties of superheavy nuclei.

A few transplutonium nuclei had been explored at the time the work described here was initiated. Ground-state rotational bands had been previously identified in a few even-even nuclei [1, 2]. K-isomeric states had not been established in any nucleus, although one in ^{254}No had been proposed earlier [3].

Most transplutonium nuclei have axial prolate shapes, and the presence of high-Ω orbitals near the Fermi surface [4] in quite a few nuclei favors robust high-K structures. Single particle energies, pairing strengths, and spin-spin residual interactions can be inferred through the identification of high-K states. Establishing prompt rotational structures up to high spins allows the exploration of moments of inertia, and additionally in odd-A nuclei, the electromagnetic properties of specific nucleonic configurations. The limit of angular momentum for the existence of discrete states, in competition with fission, also gets delineated.

2. Experiments

Nuclei with Z≥100 were populated through fusion-evaporation reactions. The cross-sections for the evaporation residues are very low, ranging from ≈2 μb for ^{254}No to 10 nb for ^{256}Rf. K isomers in ^{254}No [5] were populated using the ^{208}Pb(^{48}Ca,2n) reaction, with the mid-target energy of ^{48}Ca being 217 MeV. Beam intensities up to 120 pnA were provided by the ATLAS accelerator at Argonne National Laboratory (ANL). Separation and identification of the evaporation residues by their mass/charge ratio was achieved using the Fragment Mass Analyzer (FMA). The residues were implanted into a 140 μm thick double-sided Si strip detector (DSSD) with 40 x 40 pixels, at the focal plane of the FMA. Isomeric decays were identified by time and spatial correlations in the same pixel as the implanted nucleus. The decays typically involved γ rays, conversion electrons, and alpha particles or spontaneous fission fragments. The γ-rays from the decay of the isomer/s were recorded in clover detectors placed around the DSSD. In the experiments to study K isomers in ^{252}No [6] and ^{250}Fm [7], ^{206}Pb and ^{204}HgS targets respectively, were used. The ^{250}Fm experiment was performed at Jyväskylä, and the gas-filled separator RITU was used. In the ^{250}Fm experi-

*Electronic address: sujit@cbs.ac.in

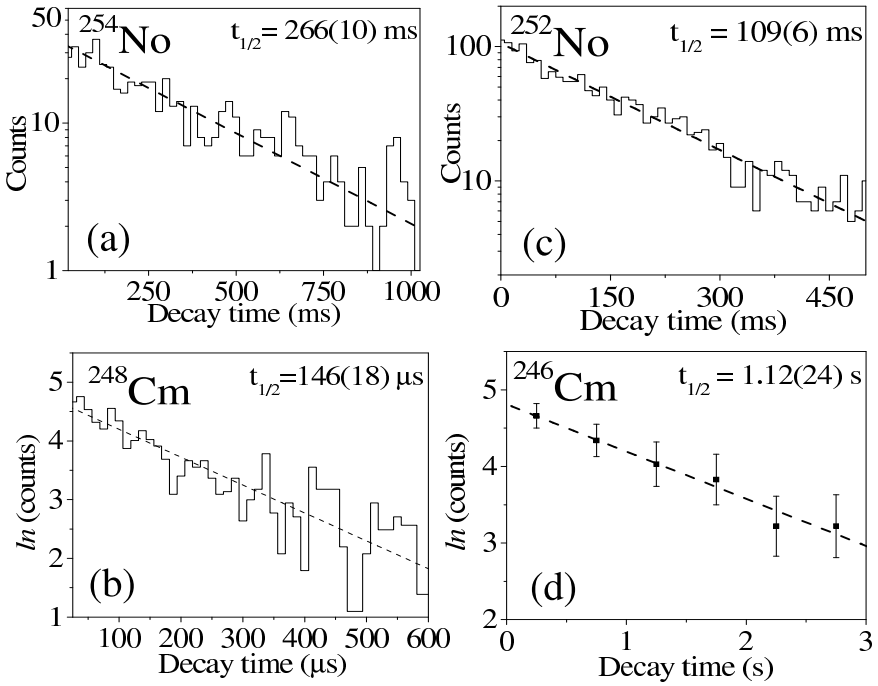

FIG. 1: (a), (b) Time distributions for the decay of the $K^{\pi}=8^{-}$ isomers in the N=152 isotones ^{254}No and ^{248}Cm. (c), (d) Same for the N=150 isotones ^{252}No and ^{246}Cm. The conversion electron and gamma-ray intensities are plotted for the No and Cm isotopes, respectively.

ment, a planar Ge detector was placed adjacent to the DSSD to record x rays and low-energy γ rays. Due to paucity of statistics of γ rays correlated with the decay of the isomer/s in the DSSD, conventional γ-γ coincidence techniques could not be used to build decay schemes. Information about the γ rays combined with the conversion electron sum energy, coincident x-ray intensities, γ energy sums and modeling of rotational bands were used to construct the decay schemes. Despite the limitations, unambiguous decay schemes for almost all isomers detected could be obtained.

It is possible to populate transplutonium nuclei with Z$\leq$98 in deep-inelastic and transfer reactions, with heavy beams incident on radioactive targets. Higher cross-sections for the reaction channels of interest can be obtained, and ancillary detectors are not required. A large array of γ detectors at the target position allows accumulation of sufficient statistics and the possibility of isolating weaker decay paths. Experiments to study K isomers in ^{248}Cf, ^{246,248}Cm, and ^{244}Pu were performed using ATLAS and Gammasphere at ANL [8]. Beams of ^{207}Pb, ^{209}Bi, and ^{47}Ti at energies around 10-15% above the barrier were delivered by ATLAS. The actinide targets had a thick ($\approx$50 mg/cm^2) Au backing and a thin ($\approx$200 μg/cm^2) Au front. Similar projectile-target combinations were used for studying prompt rotational structures in Pu, Cm and Cf isotopes.

3. K isomers

Several experiments were performed to study high-K isomeric states in transplutonium nuclei. K isomers have been identified in the N=152 isotones ^{254}No [5, 9] and ^{248}Cm [10], and the N=150 isotones ^{252}No [6], ^{250}Fm [7], ^{246}Cm [10], and ^{244}Pu [8]. A search has

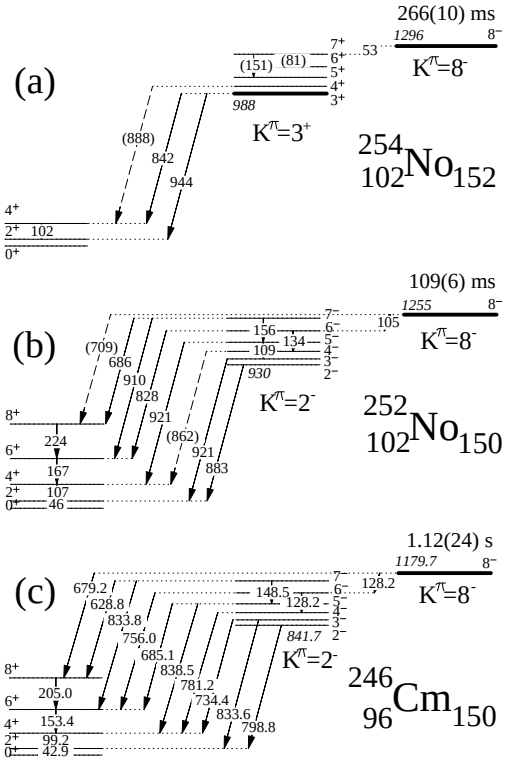

FIG. 2: Partial level schemes for the decay of $K^\pi=8^-$ isomers in: (a) ^{254}No (b) ^{252}No (c) ^{246}Cm.

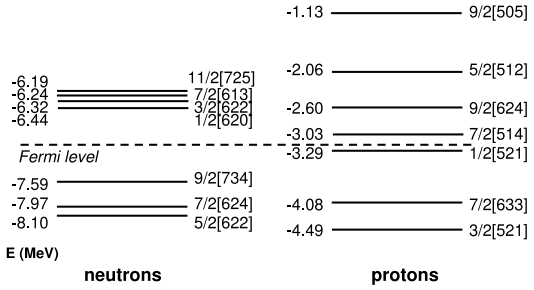

FIG. 3: Single-particle energies for ^{254}No calculated using the Woods-Saxon potential with "universal" parameters.

been performed for K isomers in ^{256}Rf [11, 12] and ^{248}Cf [8].

Two isomers have been identified in ^{254}No, with one of these having a $K^\pi=8^-$, 2-quasiparticle (qp) structure, and a half-life of 266(10) ms (Fig. 1a). For the second isomer, a half-life of 171(9) μs is deduced. Its excitation energy (≈2.6 MeV), which is about twice that of the 2-qp states, suggests a 4-qp configuration. Two-quasiproton configurations are inferred for both the $K^\pi=3^+$ and 8^- states in ^{254}No (Fig. 2a), based on the crossover-to-cascade transition intensities in the $K^\pi=3^+$ band and the observed decay from the $K^\pi=8^-$ state to the $K^\pi=3^+$ band [5]. The $K^\pi=3^+$ and $K^\pi=8^-$ states have been assigned $\pi^2([514]7/2, [521]1/2)$ and $\pi^2([514]7/2, [624]9/2)$ configurations, respectively. The [521]1/2 orbital which contributes to the $K^\pi=3^+$ configuration originates from the $f_{5/2}$ shell above the postulated Z=114 spherical shell gap.

The $K^\pi=8^-$ isomers in the N=150 isotones ^{252}No, ^{250}Fm, ^{246}Cm, and ^{244}Pu have half-lives of 109(6) ms, 1.92(5) s, 1.12(24) s, and 1.75(12) s (Fig. 1), respectively [6–8, 10]. The decay pathways are very similar for all these isomers, with one branch to a $K^\pi=2^-$ octupole vibrational band and another to the ground state band (Fig. 2b and 2c). All these isomers have identical $\nu^2([624]7/2, [734]9/2)$ configurations.

The $K^\pi=8^-$ isomer in ^{248}Cm has a half-life of 146(18) μs (Fig. 1b), with decay branches to the $K^\pi=2^+$ γ-vibrational band and the ground-state band. An experiment has been performed to search for the expected $K^\pi=8^-$ isomeric state in ^{248}Cf, and the data are being analyzed. In the case of ^{256}Rf, there are conflicting results about the presence of isomeric state/s [11, 12], and further work is required to make an unambiguous assignment.

The new isomeric states described earlier in this section have allowed a systematic comparison of the experimental energies with those predicted using different theoretical frameworks *e.g.* macroscopic-microscopic (Woods-

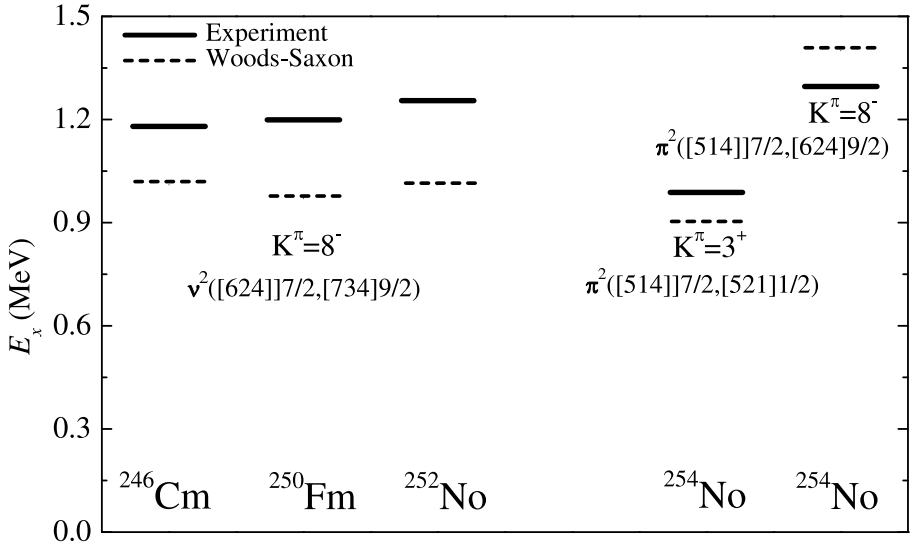

FIG. 4: Experimental and calculated energies of high-K states in No, Fm and Cm isotopes. Details about the calculations can be found in the text.

Saxon), and various density functional approaches like Hartree-Fock Bogolyubov (HFB) with the Skyrme [13, 14] and Gogny D1S interactions [15], and Relativistic Mean Field (RMF) [16].

The single-particle levels for protons and neutrons in ^{254}No, calculated using the "universal" parameterization of the Woods-Saxon (WS) potential [17] are illustrated in Fig. 3. These calculations use the Lipkin-Nogami prescription for pairing, which accounts for reduced pairing due to blocking. The WS single-particle energies give a good account of the presence of the low-energy $K^{\pi}=3^{+}$ state, since the [514]7/2 and [521]1/2 proton orbitals are very close, on either side of the Fermi level (Fig. 3).

A comparison of the calculated and experimental energies of 2-qp states for several nuclei in this region is illustrated in Fig. 4. The calculated 2-qp energies have been lowered or raised by 100 keV for spin-singlet and spin-triplet states respectively, to account for residual spin-spin interactions. It is evident that there is good agreement, to within 250 keV in all cases, although the $K^{\pi}=8^{-}$ energies are systematically underestimated for the N=150 isotones. This extends the validity of the WS energies up to Z=102. While the density functional calculations of the 2-qp energies exhibit reasonable agreement with data in some instances, in some cases there are considerable discrepancies (1 MeV or higher). This indicates that improvements are required before these models can be used to make definitive predictions of shell gaps for the heaviest nuclei. If WS energies continue to be valid in the superheavy region, then spherical magic gaps are expected at Z=114 and N=184. This is in contrast to Z=126 and N=184 predicted by Skyrme calculations, and Z=120 and N=172 from RMF. However, the reliability of extrapolating WS to even higher Z beyond No (Z=102) is unknown. The precise location of both the proton and neutron spherical shell gaps is of particular interest since it would define the center of the proposed "island of stability".

4. Prompt rotational structures

Since ground-state rotational bands in several even-even nuclei in this region had been studied earlier, most of the work described in this section was focused on the high-

spin structure of odd-A nuclei. Rotational structures built on 1-qp configurations have been identified in the odd-A nuclei ^{249}Cf and ^{247,249}Cm [18]. These constitute some of the heaviest odd-A nuclei studied up to high spins. In addition, the ground-state rotational bands in ^{248,250}Cf have been extended. Rotational bands built on the 2-qp K-isomeric states in ^{250}Fm, ^{248}Cm and ^{244}Pu have also been tentatively identified. The Pu-Cf isotopes have been investigated using deep-inelastic and transfer reactions as described earlier. Though the cross-sections are higher, strong contamination from other reaction channels like fission and Coulomb excitation of Au (which is typically used as a backing for the actinide targets) tends to dominate. Target activities also limit the feasibility of these experiments. The γ intensity in odd-A nuclei is often fragmented across multiple band structures. Low-energy transitions have a high degree of internal conversion, and there is usually insufficient information about excited states to build decay schemes through coincidences with any known γ rays. In order to enhance selectivity and enable unambiguous identification, a variety of techniques such as x-γ coincidences for Z identification, cross-coincidences with binary reaction partners coupled with band search routines were adopted. Until this work was performed, only a few odd-A transplutonium nuclei had been studied up to high spins *viz.*, ^{241}Am (Z=95), ^{251}Md (Z=101) and ^{253}No (Z=102) [14, 19–21].

High-spin ($\approx 25\hbar$) rotational bands based on the $\nu[734]9/2$ orbital of $j_{15/2}$ parentage in the N=151 isotones ^{247}Cm (Z=96) and ^{249}Cf (Z=98) were identified. In ^{249}Cm (N=153), a band built on the $\nu[620]1/2$ orbital of $2g_{7/2}$ parentage, from above the N=164 spherical sub-shell gap, has been established up to $\approx 28\hbar$. This is the highest-lying neutron configuration investigated to high spins and represents a substantial advance towards studying states close to the next predicted neutron magic shell gap. Cf is the element with the highest Z studied through inelastic excitation with a heavy-ion beam. Unambiguous

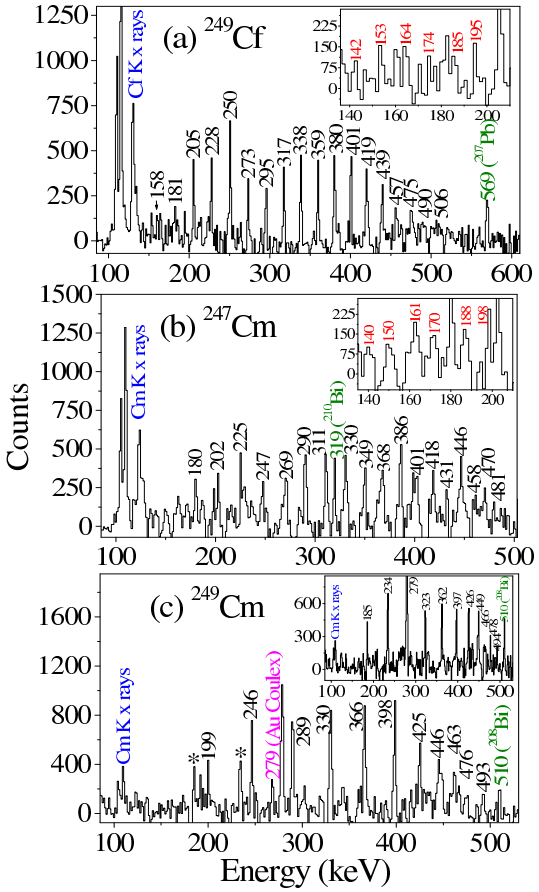

FIG. 5: Transitions in the newly established rotational structures in: (a) ^{249}Cf (b) ^{247}Cm (c) ^{249}Cm. For (a) and (b), the ΔI=2 transitions are shown in the main panel, with the ΔI=1 transitions in the inset. The transitions in the two signature partners of the rotational band in ^{249}Cm are shown in the main panel and inset of (c). The transitions marked with asterisks in (c) are observed through coincidences with the signature partner. In all the cases, the γ rays from the corresponding binary reaction partner, observed in coincidence, are indicated as well.

configuration assignments have been made using measured branching ratios. The variation with Z and N of high-spin properties has been explored.

Rotational bands have been established up to $\approx 25\hbar$ in both ^{247}Cm and ^{249}Cf. Coinci-

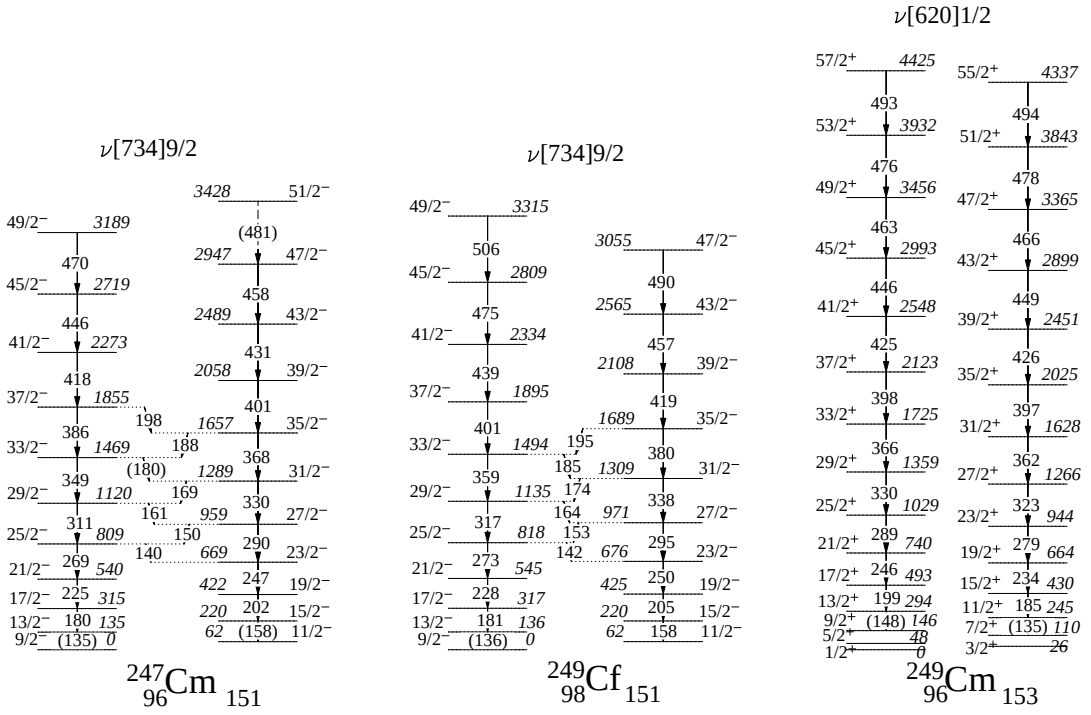

FIG. 6: The observed level structure for the $\nu[734]9/2$ bands in ^{247}Cm and ^{249}Cf, and the $\nu[620]1/2$ band in ^{249}Cm. Almost all the transitions shown above are newly observed.

dences with Cf and Cm K x rays and cross-coincidences with the 569 keV and 319 keV transitions from the lowest excited states in ^{207}Pb and ^{210}Bi (Figs. 5a and 5b), respectively, allow for an unambiguous assignment of the observed bands to ^{249}Cf and ^{247}Cm (Fig. 6). Strong coincidences between signature partners are also observed (Figs. 5 and 6). The observation of ΔI=1 transitions between signature partners (insets of Figs. 5a and 5b), in addition to the in-band E2 transitions, yields M1/E2 branching ratios. The $(g_K\text{-}g_R)/Q_0$ values (where g_K is the nucleon g factor, g_R is the rotational g factor, and Q_0 is the intrinsic quadrupole moment) extracted from the branching ratios can be compared to those expected for different Nilsson orbitals to aid configuration assignments. Values of g_R=0.31 and Q_0=12 *eb*, typical for this region, were used [22, 23]. The configuration assignments are however robust under variation of both g_R and Q_0. For the bands in ^{249}Cf and ^{247}Cm, a $\nu[734]9/2$ configuration of $j_{15/2}$ parentage is indicated, and other low-lying orbitals are ruled out, while in ^{249}Cm, the $\nu[620]1/2$ assignment is evident. The data for ^{249}Cf are shown in Fig. 7.

The similarity of MOI of the bands in ^{247}Cm and ^{249}Cf below 0.15 MeV (Fig. 8b) suggests identical configurations, and rotational parameters extracted from the newly established levels are consistent with those obtained from the known [24, 25] low-spin states based on the [734]9/2 bandhead (A≈5.7 keV, with energies E=E_0 + A $I(I+1)$). Thus far, the excitations built on the $\nu j_{15/2}$, [734]9/2 orbital were the highest-lying ones studied up to high spins in ^{253}No [20, 21]. The same orbital has now been explored in ^{247}Cm and ^{249}Cf, which are N=151 isotones of ^{253}No.

In ^{249}Cm, a band with large signature splitting, and a decoupling parameter a=0.35, is observed (Figs. 5c and 6). This value is in

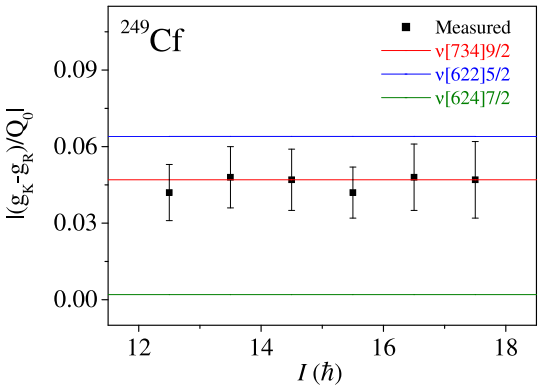

FIG. 7: Experimental (g_K - g_R)/Q_0 values for the observed band in ^{249}Cf. The data are compared with the values expected for low-lying neutron states. The ν[734]9/2 configuration is evidently favored.

agreement with a=0.33 from the known levels at low spin. Coincidences with Cm K x rays and cross-coincidences with the 510 keV γ ray from the second excited state in ^{208}Bi (Fig. 5c) allow for the band to be associated with ^{249}Cm. There are weak coincidences between the signature partners, though no ΔI=1 transitions are observed. The weaker ΔI=1 transitions are also responsible for the smaller intensity of the K x rays observed in coincidence in ^{249}Cm (Fig. 5c), as compared to ^{249}Cf and ^{247}Cm (Figs. 5a and 5b). However, M1/E2 branching ratios could be inferred for two states in the band from observed coincidences between the signature partners. The (g_K-g_R)/Q_0 values extracted from the data are consistent only with the ν[620]1/2 configuration of $2g_{7/2}$ parentage [18], which originates from above the N=164 spherical sub-shell gap.

The ground-state rotational bands in the even-even isotopes of Cf *viz.* ^{248,250}Cf have been extended up to 14$\hbar$ just below the onset of the first alignment. In ^{250}Fm, ^{248}Cm and ^{244}Pu, rotational bands built on the $K^{\pi}=8^{-}$ isomeric states have been tentatively identified. The Pu, Cm and Cf data are being further analyzed.

The investigation of isotonic (^{247}Cm, ^{249}Cf) and isotopic (^{247,249}Cm) nuclei allows an exploration of the variation of high spin properties with Z and N, in a regime where the shell-correction energy is crucial for stability against fission. These properties are described below in terms of WS cranking calculations. The calculations have been performed using the "universal" parameterization of the WS potential [17]. For each case, the deformation was fixed at the value calculated for the ground state (β_2≈0.24, β_4≈0.02-0.03, and γ=0°). Empirical values of pair gap energies were used, which were chosen to be 80% of 5-point odd-even mass differences [26]. The reduction of the pair gap energy by this amount was found to explain observed properties in the actinides better, and the extent of quenching was chosen to reproduce existing data.

For the ν[734]9/2 bands in ^{247}Cm and ^{249}Cf, the $j_{15/2}$ neutron crossing is blocked. An upbend in the experimental alignment just beyond $\hbar\omega$=0.2 MeV is observed in ^{247}Cm, and a very small increase around 0.25 MeV is seen in ^{249}Cf (Fig. 8a), which may possibly be the precursor of an alignment. For the K=1/2 band in ^{249}Cm, both $\nu j_{15/2}$ and $\pi i_{13/2}$ crossings are possible, unlike ^{247}Cm. The experimentally observed alignment gain is larger (by about 3$\hbar$) in ^{249}Cm, compared to ^{247}Cm, over the observed range of frequencies (Fig. 8a). The variation with Z of the $\pi i_{13/2}$ alignment process is also apparent through a scrutiny of the experimental kinematic moment of inertia ($\mathcal{J}^{(1)}=I/\omega$, where I is the spin and ω is the rotational frequency) for the ν[734]9/2 bands in the N=151 isotones, ^{247}Cm, ^{249}Cf and ^{253}No (Fig. 8b). At low rotational frequencies, the MOI are quite similar as a result of identical underlying configurations. The increase in MOI at higher frequencies cannot be attributed to $\nu j_{15/2}$ alignment since it is blocked. This increase is evident around $\hbar\omega$≈0.2 MeV for ^{247}Cm, around 0.25 MeV for ^{249}Cf, while there is no appreciable change in the case of ^{253}No for the observed range of frequencies.

The WS cranking calculations predict that the $\pi i_{13/2}$ crossing in ^{247}Cm, with the [642]5/2 orbital being involved, should occur at 0.22 MeV (Fig. 9a). In comparison, the calculated crossing frequency is higher for ^{249}Cf (0.25

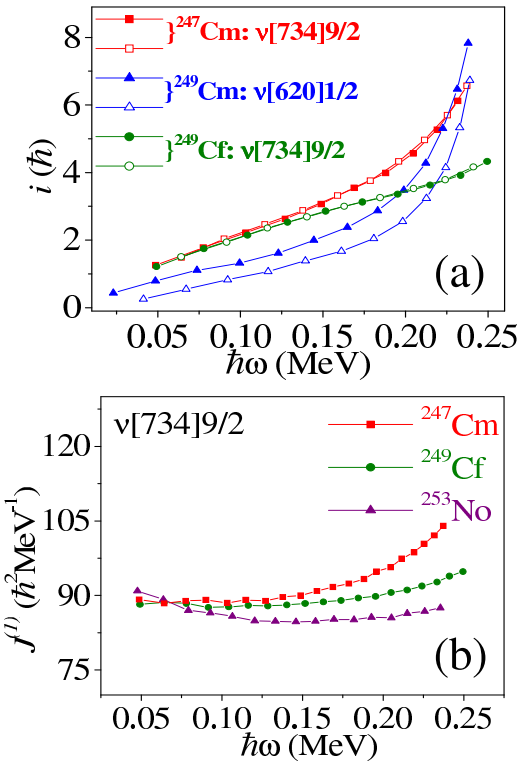

FIG. 8: (a) Alignments as a function of rotational frequency for bands in ^{247,249}Cm and ^{249}Cf. Harris parameters [27] J_0=65 $\hbar^2$MeV^{-1} and J_1=200 $\hbar^4$MeV^{-3} have been used. (b) Observed kinematic moments of inertia for ν[734]9/2 bands in N=151 isotones.

MeV), due to the presence of the higher-Ω, [633]7/2 orbital near the Fermi surface (Fig. 9b). The interaction strength at the crossing in ^{249}Cf is predicted to be significantly larger (≈0.2 MeV) than that in ^{247}Cm (≈0.07 MeV). However, it is difficult to determine whether this is the case experimentally as only the very first stage of an alignment is observed in ^{249}Cf. The predicted values for the $\nu j_{15/2}$ and $\pi i_{13/2}$ crossing frequencies in ^{249}Cm (Fig. 9c) are very similar (0.21 and 0.22 MeV, respectively). Therefore, it is reasonable to suggest that the additional alignment observed in ^{249}Cm is attributable to $j_{15/2}$ neutrons. Fig. 9d depicts a comparison of the experimental and predicted Routhians for the $j_{15/2}$ neutron band in ^{249}Cf.

While the predictions are consistent with observation, they may not necessarily offer a unique explanation. No evidence for a $j_{15/2}$ alignment has been found at N=144 and 146 [19, 23, 28, 29], even though CSM calculations predict that this should occur at $\hbar\omega$≈0.20 MeV [19], while tentative evidence for it has recently been presented for the N=142 ^{235}Np nucleus [30]. In the latter case, an alternative explanation is also possible [30]. Hence, an understanding of this possible strong neutron number dependence of the $j_{15/2}$ crossing frequency is currently not understood. The observation of a rotational band built on a $j_{15/2}$ neutron configuration in ^{249}Cm could possibly help establish with more certainty whether or not the expected $j_{15/2}$ alignment is observed at N=153, provided this collective sequence can be established to sufficiently high spins.

This work provides the first detailed information on high-spin collective structures in several odd-A nuclei near the region where shell effects are responsible for stability. The ν[734]9/2 and ν[620]1/2 orbitals are the highest-lying neutron configurations investigated thus far up to high spin, with the [620]1/2 state being from above the N=164 sub-shell gap. The underlying nucleonic configurations have been inferred from measured branching ratios. The variation of collective properties with both proton and neutron number has been investigated. Cranking calculations using the universal parameterization of the Woods-Saxon potential and a quenched, empirical pair-gap energy describe most of the observed properties, but there is no consistent explanation for the absence of alignment of $j_{15/2}$ neutrons in several nuclei. Calculations using self-consistent mean-field approaches for the heaviest odd-A nuclei accessible to spectroscopy are required for discriminating between and possibly improving available approaches and interactions. More sensitive experiments to investigate odd-A transfermium nuclei are on the horizon, and will add to existing sparse data and contribute to the refinement of theoretical descriptions of the heaviest nuclei.

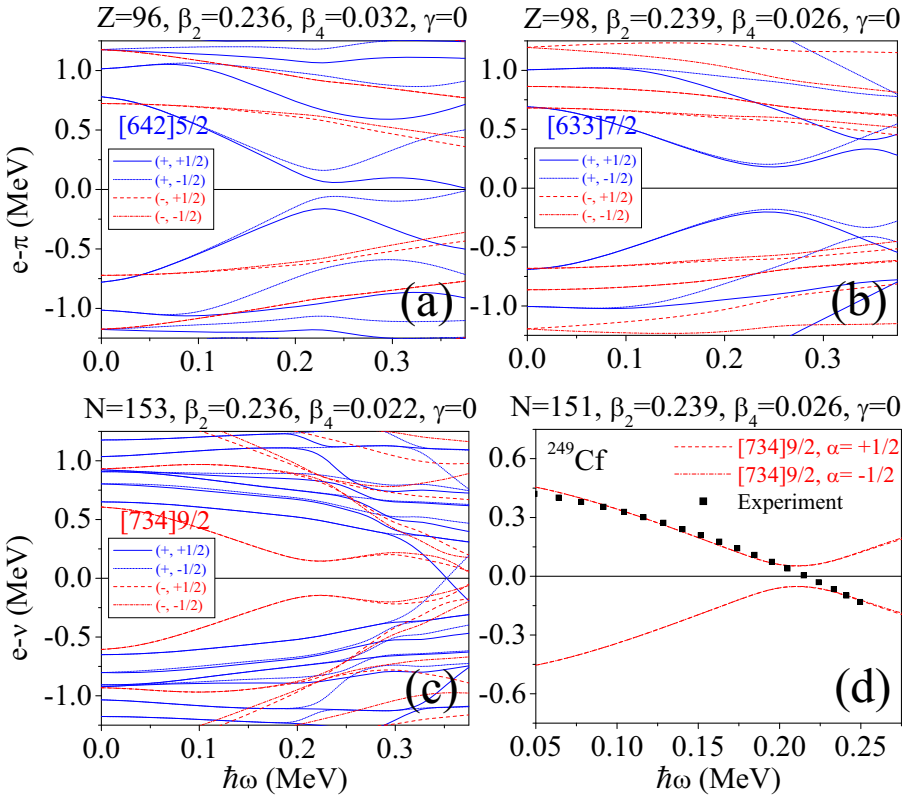

FIG. 9: Quasiparticle levels from Woods-Saxon cranking calculations: (a) Protons in ^{247}Cm (b) Protons in ^{249}Cf (c) Neutrons in ^{249}Cm (d) Calculated and experimental Routhians for the [734]9/2 neutron orbital in ^{249}Cf. The experimental energy has been offset by an arbitrary amount.

Acknowledgments

I would like to thank all my collaborators at Argonne National Laboratory, University of Massachusetts Lowell, University of Jyväskylä, University of Liverpool, the United States Naval Academy and elsewhere for their dedicated efforts in the realization of various aspects of this work. This research was supported by the U.S. Department of Energy, Office of Nuclear Physics, under Grants DE-FG02-94ER40848 and DE-AC02-06CH11357, and the National Science Foundation. The author is also indebted for the use of ^{248}Cm and ^{249}Cf to the Office of Basic Energy Sciences, U.S. Department of Energy, through the transplutonium element production facilities at Oak Ridge National Laboratory.

References

[1] P. Reiter *et al.*, Phys. Rev. Lett. **82**, 509 (1999).
[2] R.-D. Herzberg *et al.*, Phys. Rev. C **65**, 014303 (2001).
[3] A. Ghiorso *et al.*, Phys. Rev. C **7**, 2032 (1973).
[4] R. Chasman *et al.*, Rev. Mod. Phy. **49**, 833 (1977).
[5] S.K. Tandel *et al.*, Phys. Rev. Lett. **97**, 082502 (2006).
[6] A.P. Robinson *et al.*, Phys. Rev. C **78**, 034308 (2008).
[7] P.T. Greenlees *et al.*, Phys. Rev. C **78**, 021303(R) (2008).
[8] S.K. Tandel *et al.*, unpublished.
[9] R.-D. Herzberg *et al.*, Nature (London)

442, 896 (2006).
[10] U.S. Tandel *et al.*, Proc. of Nuclear Structure 2008, East Lansing, Michigan.
[11] A.P. Robinson *et al.*, Phys. Rev. C **83**, 064311 (2011).
[12] H.B. Jeppesen *et al.*, Phys. Rev. C **79**, 031303(R) (2009).
[13] M. Bender *et al.*, Nucl. Phys. A **723**, 354 (2003).
[14] A. Chatillon *et al.*, Phys. Rev. Lett. **98**, 132503 (2007).
[15] J.-P. Delaroche *et al.*, Nucl. Phys. A **771**, 103 (2006).
[16] A.V. Afanasjev *et al.*, Phys. Rev. C **67**, 024309 (2003).
[17] S. Ćwiok *et al.*, Comp. Phys. Comm. **46**, 379 (1987).
[18] S.K. Tandel *et al.*, Phys. Rev. C **82**, 041301(R) (2010).
[19] K. Abu Saleem *et al.*, Phys. Rev. C **70**, 024310 (2004).
[20] P. Reiter *et al.*, Phys. Rev. Lett. **95**, 032501 (2005).
[21] R.-D. Herzberg and P.T. Greenlees, Prog. Part. Nucl. Phys. **61**, 674 (2008).
[22] K. Abu Saleem, PhD thesis, Illinois Institute of Technology, Chicago, USA, 2002.
[23] S. Zhu *et al.*, Phys. Lett. B **618**, 51 (2005).
[24] S.W. Yates *et al.*, Phys. Rev. C **12**, 442 (1975).
[25] I. Ahmad *et al.*, Phys. Rev. C **68**, 044306 (2003).
[26] P. Moller and J.R. Nix, Nucl. Phys. A **536**, 20 (1992).
[27] S.M. Harris, Phys. Rev. 138, B509 (1965).
[28] I. Wiedenhöver *et al.*, Phys. Rev. Lett. **83**, 2143 (1999).
[29] X. Wang *et al.*, Phys. Rev. Lett. **102**, 122501 (2009).
[30] A.M. Hurst *et al.*, Phys. Rev. C **81**, 014312 (2010).